Photodiagnosis and Photodynamic Therapy 28 (2019) 238–247

Contents lists available at ScienceDirect

Photodiagnosis and Photodynamic Therapy

journal homepage: www.elsevier.com/locate/pdpdt

Biosensor device for the photo-specific detection of immuno-captured bladder cancer cells using hexaminolevulinate: An *ex-vivo* study

Kit Man Chan[a], Krasimir Vasilev[b], Hanieh Safizadeh Shirazi[b], Kym McNicholas[d], Jordan Li[c,d], Jonathan Gleadle[c,d], Melanie MacGregor[b,*]

[a] School of Engineering, University of South Australia, South Australia, Australia
[b] School of Engineering, Future Industries Institute, University of South Australia, South Australia, Australia
[c] Department of Renal Medicine, Flinders Medical Centre, Bedford Park, South Australia, Australia
[d] College of Medicine and Public Health, Flinders University, Bedford Park, South Australia, Australia

ARTICLE INFO

Keywords:
Bladder cancer
Urine
Non-invasive
5-Aaminolevulinic acid
Photodynamic diagnosis
Hexaminolevulinate

ABSTRACT

Exogenous administration of the photodynamic agent hexaminolevulinate induces Protoporphyrin IX (PpIX) accumulation in malignant tissue. This may enable differentiation from healthy tissues by emission of a distinctive red fluorescence. It provides the photo-specific detection when excited with blue light at 405 nm. This study determines the *ex-vivo* processing conditions (time, concentration, temperature and addition of a fluorescent dye) required for HAL-induced PpIX fluorescence to successfully discriminate between bladder cancer and benign fibroblast cells shed in urine at the single cell level. HAL-induced fluorescence was 4.5 times brighter in cancer cells than non-cancer cells when incubated in the optimum conditions, and could be used to correctly identified bladder cancer cells captured within a newly developed immunofunctionalized biosensor with 88% efficiency. This biosensor is designed to facilitate the immuno-capture of cancer cells by interaction with carcinoma specific anti Epithelial Cell Adhesion molecule (anti-EpCAM) antibodies. Anti-EpCAM antibodies were immobilized on polyoxazoline (POx) plasma polymers by covalent bonds in microfluidic channels. Combining photodynamic and immunoselective approach therefore constitute a promising approach for the non-invasive diagnosis of bladder cancer with two independent level of confidence.

Objective: This study investigate the relationship between different regulatory factors (time, concentration, temperature and addition of a fluorescent dye) and Hexaminolevulinate (HAL)-mediated photodynamic diagnosis of bladder cancer (PDD) *in vitro*. We examine the natural photosensitizer Protoporphyrin IX (PpIX) fluorescence induced by HAL in several human bladder cancer cell lines and one non-cancer foreskin fibroblast cell line and identify the processing conditions that maximise the difference in fluorescence intensity between malign and benign cell types. The detection of HAL induced fluorescence at a single cell level by a selective cancer cell capture platform is also tested.

Materials and methods: Experiments were performed on cultured monolayer cells and cells in suspension. The cell lines examined included the transitional epithelium carcinoma cell lines HT1197, HT1376, EJ138 and RT4, and the non-cancer foreskin fibroblasts HFF. Cells were incubated with HAL in various doses, time and temperature settings. We also used the nuclear red as a tool to study the PpIX subcellular localization. PpIX fluorescence intensities were measured and analysed using fluorescence microscope software. Finally, we evaluated the possibility of using HAL to discriminate between cancer and non-cancer cells from a mixed cell population using a newly developed immunofunctionalized microfluidic platform.

Results: The accumulation of PpIX in bladder cancer cells was significantly higher than in non-cancer cells, both cultured monolayer cells and cells in suspension. Effectively, the fluorescence intensity was 4.5 times brighter in bladder cancer cells than non-cancer foreskin fibroblast cells when incubated in the optimum condition, in which the nuclear stain adjuvant acted as a fluorescence enhancer. Cancer cells displayed PpIX accumulated mainly in mitochondria but none or very little PpIX was observed in non-cancer cells. HAL-induced fluorescence could be used to correctly identify bladder cancer cells within the EpCAM conjugated POx based microfluidic sensor with

* Corresponding author.
E-mail addresses: kit_man.chan@mymail.unisa.edu.au (K.M. Chan), krasimir.vasilev@unisa.edu.au (K. Vasilev), hanieh.safizadehshirazi@unisa.edu.au (H.S. Shirazi), kym.mcnicholas@flinders.edu.au (K. McNicholas), jordan.li@sa.gov.au (J. Li), jonathan.gleadle@sa.gov.au (J. Gleadle), melanie.macgregor@unisa.edu.au (M. MacGregor).

https://doi.org/10.1016/j.pdpdt.2019.08.001
Received 16 May 2019; Received in revised form 20 July 2019; Accepted 2 August 2019
Available online 05 August 2019

an 88% capture selectivity rate.
Conclusions: These findings prove that the application of HAL-induced PpIX fluorescence can successfully distinguish between cancer and non-cancer cells *in vitro*. This test can provide advanced second level of confidence on the cancerous nature of cells captured by the immunofunctionalized bladder cancer diagnostic platform.

1. Introduction

Bladder cancer is one of the most common forms of cancer diagnosed worldwide. In the United States, it is the seventh most common cause of cancer death [1] with 60,000 new cases and 12,000 deaths occurring in 2017 [2]. Cancers of the urinary bladder are usually urothelial carcinomas, and most patients are diagnosed with low grade non-muscle invasive bladder cancer (NMIBC), which has a high recurrence rate of 70%. Additionally, 50% of NMIBC are likely to progress to the more aggressive and higher grade muscle invasive bladder cancer (MIBC) [3].

For this reason bladder cancer survivors have to undertake frequent follow up tests for the rest of their lives. The nature of the follow-up tests currently used in clinical practice has earnt bladder cancer the title of most expensive cancer to treat from diagnostic to death per capita [4]. Cystoscopy, the current gold standard diagnostic method, is invasive, costly and often fails to detect flat lesions [5]. The most common non-invasive test is cytology, which has disappointingly low sensitivity rates [6]. While several other non-invasive approaches have been proposed over the years, they have not proven accurate enough to supplant cystoscopies. Hence, improved non-invasive diagnostic methods for use in long term surveillance still need to be developed to improve bladder cancer management.

A significant increase in urinary bladder cancer detection rate, and in particular urothelial neoplastic lesions, was achieved by the introduction of Photodynamic diagnosis (PDD) using 5-aminolevulinic acid (5-ALA)-assisted cystoscopy [7,8]. PDD uses a photosensitizer which, when triggered with a light source of the right wavelength, emits a cancer specific fluorescence in tumour tissues. 5-ALA is a natural amino acid synthesized from succinyl-CoA and glycine in haem biosynthesis. 5-ALA does not fluoresce, but is a precursor of the natural photosensitizing metabolite, protoporphyrin IX (PpIX) [9–11]. Exogenous administration of 5-ALA increases the accumulation of PpIX primarily in tumour tissues. When excited with blue light at 405 nm wavelength, tumour cells emit a bright red fluorescence at 620 nm, reportedly several fold brighter than normal healthy cells [12,13]. The use of this particular light wavelength is the core concept of “photospecific detection”.

Kriegmair and his colleagues [7] introduced the use of exogenous 5-ALA administration by instillation or ingestion in bladder cancer patients, followed by blue light cystoscopy. This technique proved to be more sensitive than white light cystoscopy when applied to high grade flat tumours which are otherwise missed easily [14,15]. Hexaminolevulinate (HAL) is the most successful and common use of 5-ALA derivative [16], and has been approved for *in vivo* photodynamic detection of bladder cancer by the FDA and European Union. It has been reported to increase PpIX fluorescence intensity in lower concentrations and with shorter exposure than 5-ALA itself [17,18]. HAL being more lipophilic than 5-ALA [19], its cellular uptake through the plasma membrane is greater. HAL-mediated fluorescence cystoscopy significantly improves bladder cancer detection in clinical practice [20]. For these reasons, the potential of 5-ALA and its derivatives as fluorescent photosensitizers for the PDD of bladder cancer *ex vivo* has since been investigated [21–23]. Several research groups have reported that the fluorescence intensity of cancer cells was higher and stronger than normal cells after HAL incubation. [21,24].

Nonetheless, there are still limitations to the use of 5-ALA and its derivatives for bladder cancer diagnosis in voided urine samples. These include the non-specific fluorescence displayed by urinary bacteria after 5-ALA incubation [25], the presence of a significant number of background cells and urine metabolites [26] in conjunction with the low number of cancer cells actually being shed in urine; as well as lengthy sample processing. The problem of non-specific fluorescence of bacteria may be partially resolved by using HAL instead of 5-ALA. Indeed, Fotinos et al. indicated that no fluorescent porphyrins were produced by bacteria when HAL is used [25]. This finding has since been supported by Nakai et al. [24]. The rarity of cancer cells shed in urine is a challenge that could be successfully addressed by cell enrichment technologies, such as microfluidic devices designed to selectively immobilise cancer cells from mixed cells population in suspension [27]. Such enriching microdevices used in combination with novel markers like HAL, could significantly improve the sensitivity of cancer detection in urine, potentially down to single cell sensitivity. Furthermore, as established for blue light cystoscopy, HAL proved to be superior over 5-ALA in *ex vivo* [24] setting due to its high lipophilicity. As a result, lower dosage and shorter incubation time are needed, and to achieve higher PpIX fluorescence selectivity in tumour cells [16,28].

We previously reported on a novel microfluidic approach for the non-invasive selective capture of cancer cells in voided urine [27]. Carcinoma specific Epithelial Cell Adhesion molecule (EpCAM) antibodies were immobilized on polyoxazoline (POx) plasma polymers by covalent bonds in microfluidic channels [29–31]. The anti-EpCAM functionalized POx film facilitates the direct selective immuno-capture of cancer cells by EpCAM antibodies in urine samples. Here we propose to use this technology in conjunction with HAL based photodynamic detection to add an additional level of confidence in detecting the presence of bladder cancer cells in urine. In this work we study the HAL-induced PpIX fluorescence in several human bladder cancer and non-cancer control cell lines with the aim to maximise the difference in fluorescence intensity between malignant and benign cell types. Different variables such as time, concentration and temperature were tested as well as the addition of another fluorescent dye adjuvant to identify optimum condition for HAL-mediated PDD *ex vivo* for the identification of cancer cells selectively captured in immunofunctionalised microfluidic devices.

2. Materials and methods

2.1. Cell culture

Human foreskin fibroblasts (HFFs) (Cell Lines Service, DKFZ, Germany) were cultured in Dulbecco’s Modified Eagles Medium (DMEM) (Life Technologies, Australia) supplemented with 10% (v/v) fetal calf serum, 100 IU/mL penicillin, 100 µg/mL streptomycin and 1% L-glutamine (200 mM). Four human Caucasian bladder transitional-cell carcinoma cell lines were obtained from European Collection of Authenticated Cell Cultures (ECACC). EJ138 (No. 85061108); HT 1376 (No.87032402); HT 1197 (No.87032403) and were cultured in

Minimum Essential Medium Eagle (MEME) (Sigma-Aldrich, Australia) with the same supplements as above as well as 1% 100x MEM Non-essential Amino Acid Solution. RT4 (No. 91091914) was cultured in McCoy's 5A medium (Sigma-Aldrich, Australia) with the same supplements as above. All cells were cultured at 37 °C with 5% CO2 in a humidified atmosphere. Cells viabilities were measured with an automated cell counter LUNA-II™ (Logos Biosystems, South Korea) after staining with trypan blue.

2.2. Chemicals

Hexaminolevulinate (HAL) hydrochloride and phosphate-buffered saline (PBS) tablets were purchased from Sigma-Aldrich (NSW, Australia). HAL was supplied as a powder and was dissolved in PBS to different concentrations from 0 to 250 μM. Nuclear red™ LCS1 (Cat# 17542),a cell-permeant nucleic acid detection dye, was obtained from AAT Bioquest® (CA 94085, USA). Dimethylsulphoxide (DMSO) was used as a reconstitution solvent for Nuclear red™ LCS1 stock solution. Polyclonal goat anti-human EpCAM antibody (AF960) was purchased from R&D Systems. Chemicals were stored in aliquots at -20 °C until use.

2.3. PpIX fluorescence microscopy

2.3.1. Cell monolayer in vitro

Cells were seeded in 96-well plates (Corning, NY) and cultured at different time points in serum-free culture medium containing different concentrations of HAL (0–250 μM) for 2 to 24 h (Fig. S1) at 37 °C. Serum-free media is necessary because lipophilic fluorescent PpIX diffuses out of the cells faster in culture media containing serum [32]. The 96-well plates were kept in a CO2 incubator for the whole incubation period. After incubation, the HAL containing medium was discarded and the cells washed with PBS (Fig. 1a).

PpIX intensity was measured using a custom made inverted fluorescent microscope (Olympus, IX83, Japan) in which the light excitation wavelength was set to 405 nm and emission wavelength to 600 nm, using a specially designed filter cube (Chroma) and an Operetta high-content imaging system (PerkinElmer Inc. USA).

2.3.2. Cells in suspension

Cells were removed from the culturing flasks after trypsinization, then resuspended in the serum-free medium to dilute the trypsin and adjusted to the targeted cell density. The cells in suspension were incubated in the dark from 30 min to 6 h with serum-free mediums containing different concentrations of HAL at 37 °C in a humidified 5% CO2 incubator. After incubation, the cells were centrifuged at 1500 rpm for 5 min. and the HAL containing medium discarded. Cells were resuspended with PBS, and 100 μl per well was aliquoted into 96-wells plates.

PpIX fluorescence was imaged using appropriate LED lamps and custom filters, referred to as PpIX optical channel in the following. Images at x 5 magnification were recorded and the fluorescence intensity measured using CellSens software (Olympus, Japan). Fluorescence images were captured and used for visualizing the cellular localization of PpIX.

2.3.3. Temperature

To evaluate the effect of temperature on PpIX fluorescence, cells were stored in the dark at different temperature settings (4 °C, RT ~23 °C, and 37 °C) in closed test tubes following the exogenous HAL incubation from 30 min to 2 h with PBS, following steps as described above in "Cells in suspension" section.

2.3.4. Nuclear red

Human bladder cancer cells HT1376 and non-cancer foreskin fibroblasts cells HFF were incubated in the dark at 37 °C with 0, 10, 50 and 100 μM HAL in serum-free medium for 1 and 2 h. Cells were then centrifuged, and HAL-containing medium decanted before incubating for another 15 min with nuclear red stain diluted in DMSO. Prior to imaging, cells were washed with PBS twice. Nuclear Red fluorescence was imaged using appropriate LED lamps and custom filters, referred to as Cy5 optical channel in the following.

2.4. Cell capture

2.4.1. Plasma surface deposition

Polymethylmethacrylate (PMMA) slides with 3 microchannels grooves were coated with a plasma deposited oxazoline thin films using a custom made parallel plate plasma reactor, as described previously [27]. 2-methyl-2-oxazoline (Sigma Aldrich Australia) precursor was introduced in the reactor with a $1.3e^{-1}$ mbar working pressure. The plasma was ignited for 3 min with a continuous radiofrequency power of 50 W. The coated microfluidic chips were kept in the dark under vacuum until further use [33].

2.4.2. Functionalization of the polyoxazoline-coated substrate

One microchannel of the POx coated slides is used unmodified as positive control. POx biocompatibility [29] allows non-specific attachment of all cell types. The test channel was functionalized with anti-EpCAM antibodies (EpCAM). The anti-EpCAM antibody solution (60 μL of 10 μg/mL in PBS) was added to the microchannel and stored in 4 °C overnight for binding. The microchannel slide was then incubated at 37 °C for 1 h, before adding 1 mg/mL skim milk solution to block the remaining POx surface for 45 min. The last microchannel was also blocked with 1 mg/mL skim milk solution, to be used as a negative control on which cell binding is inhibited. The microchannels were gently rinsed with PBS three times to remove any unbound protein and fresh PBS was added.

2.4.3. Selective cancer cell capture assay

Both Non-cancer foreskin fibroblast HFF and bladder cancer HT1376 cells were incubated in suspension with 50 μM HAL at 37 °C for first 30 min. and 23 °C for the next 30 min.. Cancer HT1376 cells were stained with 0.25 μM nuclear red for 10 min.. The cell densities of both cell lines were adjusted to range between 2×10^5 to 3×10^5 cells per mL, then mixed together in 1:1 ratio. 50 μL of the mixed cell solution was pipetted into each microchannel for fluorescence imaging. After 45 min, unbound cells were rinsed off with fresh PBS in all microchannels and the surfaces were imaged a second time. The fluorescence micrographs were used to determine the number of cell captured and PpIX fluorescence intensities.

2.4.4. Statistical analysis

Mean values and standard deviation (SD) of fluorescence intensity value for each concentration at each time point were calculated and analysed for each cell line. The student's *t*-test (GraphPad and Minitab 18 software) was used to establish the significance of differences. Statistical significance was considered as $p < 0.05$.

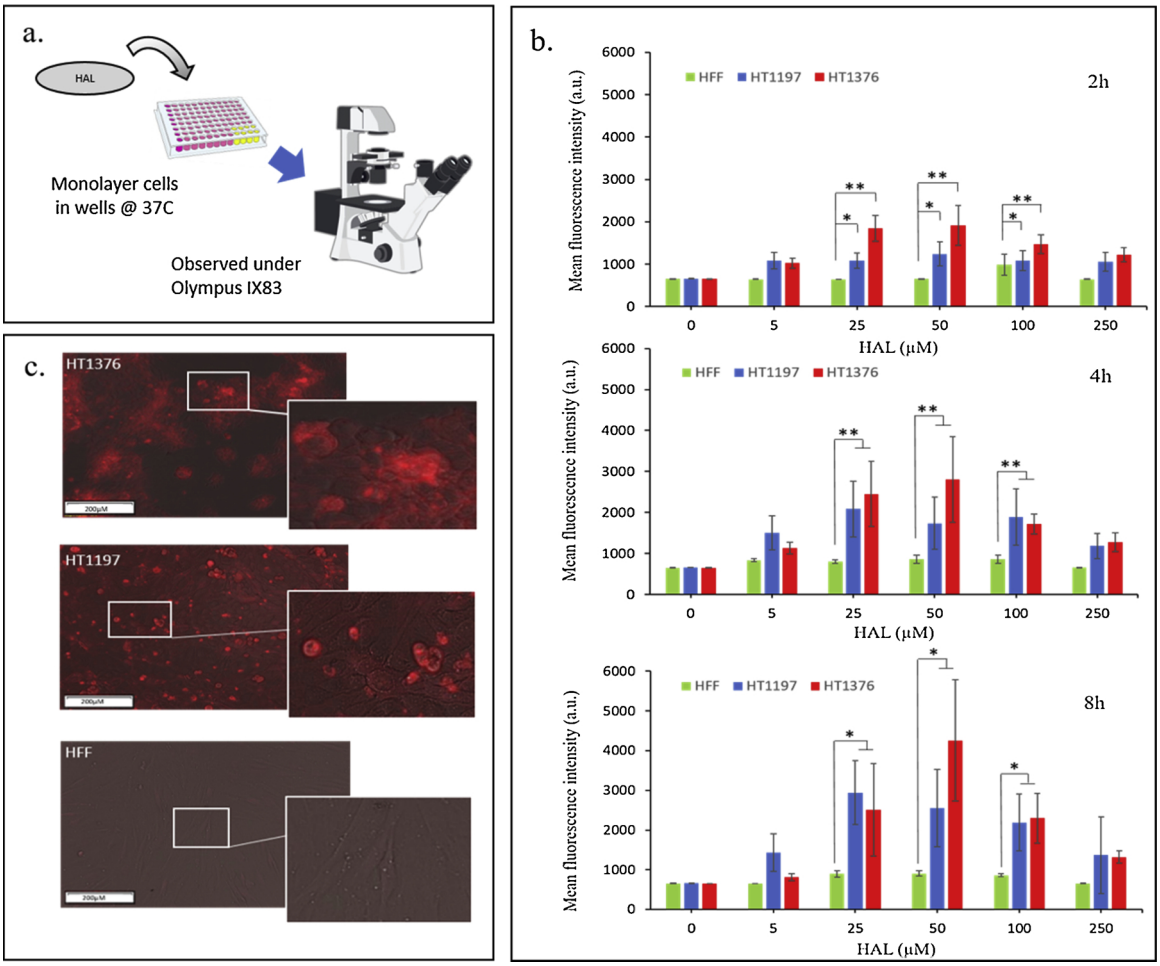

Fig. 1. Effect of time and concentration on the 5-ALA induced fluorescence of cell monolayers. a) Schematic of the monolayer *in vitro* experiment. b) time-dependent and concentration-dependent graphs of mean fluorescence intensities accumulated in different cell lines after incubation with various concentrations of HAL. c) intracellular localization of PpIX in bladder cancer cells (HT1376 and HT1197) and non-cancer cells (HFF) after incubation with 50 μM HAL for 6 h. Bright red fluorescent observed in both cancer cells but none in non-cancer cells under fluorescence microscopy, magnification 10 × . Brackets: * $p < 0.05$; ** $p < 0.01$; *** $p < 0.001$.

3. Results and discussion

3.1. PpIX fluorescence in cell monolayers in vitro

Both bladder cancer cells lines monolayers (HT1197 and HT1376) displayed a bright red fluorescence when incubated with serum-free mediums containing various concentrations (10–250 μM) of HAL over 2 to 24 h incubation period. The differences in PpIX fluorescence intensity and intracellular localization of PpIX in each cell monolayers are shown in Fig. 1b and 2c. While the fluorescence intensities did not show much difference between 25 to 100 μM in most cell lines, HT1376 performed better at 50 μM in some conditions (Fig. 1b and S1). Non cancer foreskin fibroblast HFF cells had lower PpIX fluorescence intensity than the cancer cells which remained rather constant for all HAL concentrations and incubation times. In contrast, the mean fluorescence intensities of cancer cell lines HT1197 and HT1376 demonstrated a time- and concentration-dependent pattern. The HAL-induced PpIX fluorescence in HT1197 and HT1376 increased with time from 2 to 8 h before decreasing from the 10.5 h time point (Fig. S1). A comparable time dependence was observed for two additional bladder cancer cell lines EJ138 and RT4 (Fig. S1), we can see variations in between cell lines at different HAL incubation time and concentration, which indicate that the HAL-induced PpIX production is a complex, dynamic mechanism. As we recently reviewed (*"In order for the light to shine so brightly, the darkness must be present*- Why do cancers fluoresce with 5-aminolaevulinic acid? *Francis Bacon (1561–1626), K. McNicholas et al, British Journal of Cancer, in press*). Further investigations, beyond the scope of this work, are underway to try and give elements of response to this question.

This trend was independent from the imaging systems used to measure the fluorescence intensity. (Fig. S2) Furthermore, the fluorescence intensity was greatest for HAL concentrations between 25 to 100 μM. Lower HAL concentrations did not induce significant PpIX biosynthesis in the cancer cells compared to the healthy foreskin fibroblast HFF cells. On the other hand, HAL concentrations higher than 100 μM seemed to initiate cytotoxicity and damage to the cells as noted by a decrease in fluorescence intensity and the formation of extracellular vesicles (Fig. S3). Again, the observed trends in fluorescence intensity were consistent amongst all bladder cancer cell lines and all instruments, thus confirming the robustness of the findings (Fig. S1 and S2). Finally, HAL-induced fluorescence of the cancer cell monolayer was tested on difference cell growth substrates, namely plasma POx coated and non-coated microfluidic channels, Fig. S4. Again, the fluorescence intensity of cancer cells was higher than that of healthy cells and it increased with time just the same as on tissue culture plate. From these results, we deemed the HAL concentrations of 50 and 100 μM to be the optimum for further experiments. The patterns of intracellular PpIX localization (Fig. 1c) observed by fluorescence microscopy were different between bladder cancer H1197 and HT1376 cells. PpIX was not only visible in discreet cell organelles but also extended to the

cytoplasm and nuclear region. Fluorescence in HT1376 and HT1197 cancer cells was also distributed in a few very bright red spots and in the plasma membrane.

It is also worth noting that PpIX production by exogenous HAL administration was found to be a cell density dependent phenomenon in the monolayer configuration. The PpIX fluorescence increased with increasing monolayer cell numbers, in agreement with previous studies [8,34,35]. It is well known that cancer cells tend to grow and divide densely which increases their cell to cell interaction [34]. One manifestation of this cancer specific behaviour is an increased intercellular sharing of metabolites such as ions, molecules and likely in this case, PpIX [35].The HAL-induced PpIX molecules are synthesized in the mitochondria *via*the haem biosynthesis pathway. ABCG2 exports PpIX from the mitochondria to the cytosol and reduced ABCG2 levels have been reported to boost PpIX fluorescence in human bladder cancer T24 and human histiocytic lymphoma U937 cells [36]. Some studies have pursued the role of other membrane transporters such as heme exporter feline leukemia virus subgroup C receptor (FLVCR) and translocator protein (TSPO) on PpIX intra and intercellular transport. Rosenberg et al. showed that the suppression of TSPO protein can cause PpIX accumulation [37], while others have demonstrated that PpIX can be exported out of the cells by FLVCR1 [38]. The presence of PpIX fluorescence in the cytoplasm and along the intercellular space observed here for HT1376 and HT1197 cell lines therefore warrant further investigation as it could be indicative of enzymatic activity and/or protein expression level unique to cancer cells.

3.2. PpIX Fluorescence in cells in suspension

The purpose of our current studies is to evaluate the feasibility of HAL for the fluorescently-assisted detection of cancer cells in patient urine samples. For the non-invasive diagnostic of bladder cancer, HAL would be applied to urine samples in which cancer cells are be shed. In this practical situation, the cancer cells are not in the form of an ideal monolayer, but rather are dispersed in suspension. To test the real use scenario as accurately as possible we used cells in suspension for further experiments. Also, in an effort to mimic realistic time and reagent constraints, we tested a lower HAL concentration range (0–150 μM) and extended the investigation towards shorter incubation time (0.5–6 h).

A significant increase of PpIX fluorescence intensities in cells in suspension was observed when compared to monolayer cells. This could be due to the additional cell surface area available to uptake HAL for cells in suspension. At comparable incubation time (2 h) and HAL concentration (50 μM) the fluorescence of cancer cells in suspension was three time higher than that of cell monolayers. This result indicates that HAL-induced fluorescence is particularly well suited for use in voided urine samples containing suspended malignant cells. The accumulation of PpIX increased in a time-dependent manner for both cancer

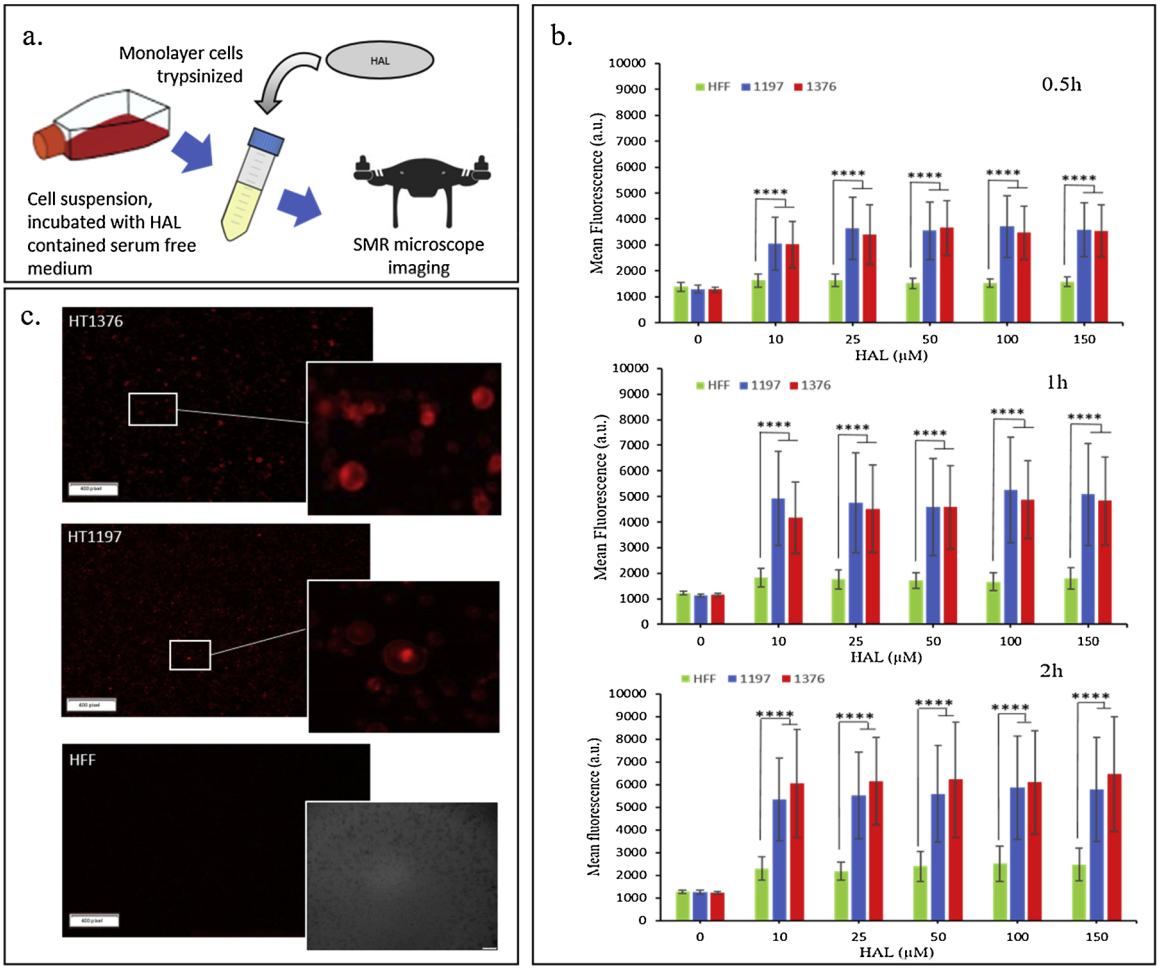

Fig. 2. Effect of time and concentration for cells in suspension. a) Schematic of the experiment. b) time-dependent and concentration-dependent graphs of PpIX accumulated in different cell lines after incubation with various concentrations of HAL. c) intracellular localization of PpIX in bladder cancer cells (HT1376 and HT1197) and non-cancer cells (HFF) after incubation with 50 μM HAL for 1 h. Bright red fluorescent observed in both cancer cells but none in non-cancer cells under fluorescence microscopy, magnification 5 × . Brackets: **** $p < 0.0001$.

cells HT1197 & HT1376. The absolute fluorescence intensity for cancer HT1376 cells increased with time from 3500 a.u. at 0.5 h to 6000 a.u. at 2 h. Non-cancer foreskin fibroblast HFF cells expressed a slight increase in the PpIX level over 2 h HAL incubation but not at 0.5 h and 1 h. No significant difference in fluorescence emission was observed over the range of HAL concentrations investigated (10 μM to 150 μM). For all cell lines in suspension PpIX fluorescence is time dependent but seemingly not dose independent. Similar to the monolayer configuration, the fluorescence intensities variance from the mean was greater for longer HAL incubation time in cancer cells (Fig. 2b and S5). Overall, the difference of mean fluorescence intensities between both cancer cells lines and non-cancer cells is statistically significant ($p < 0.0001$).

Based on our data as depicted in Fig. 2b. Also, here we used 10^5 cells on average but we know that in some cases patient urine sample cellularity is much higher than that, and so, although 25 μM maybe sufficient for cell line experiments. We decided to choose 50 μM to guarantee excess HAL will be available for future practical applications. And propose that the optimum condition for diagnostics with 1 h–2 h incubation.

3.3. Effect of temperature

PpIX is synthesized through the heme biosynthesis pathway. This multi-step process, can be affected by many factors, including temperature. Tumours have a higher temperature compared to neighbouring normal tissues [39,40] and studies have shown that more cellular PpIX is formed at higher temperatures in human cells [41,42]. This is because the heme biosynthesis is an enzymatic process and the rate of enzymatic activities increases as the temperature is raised, until the optimum temperature of around 37 °C in human cells [41,43]. This cancer specific phenomenon is readily used in blue light cystoscopy for the identification of tumors *in situ.* To determine if temperature would be a factor affecting the PpIX fluorescence *ex situ*, we used the same experimental setup as for cells in suspension but incubated the cells in HAL at 4 °C and room temperature of 23 °C instead of 37 °C. Our data (Fig. 3 and S7) indicates that the cancer specific PpIX fluorescence is not only dependent on HAL incubation time but also temperature. The PpIX fluorescence intensities of HT1376 cells incubated at 23 °C was comparable to that observed at 37 °C, and significantly brighter than in healthy cells. However, for incubation conducted at 4 °C, the fluorescence in the cancer cells was just as low as that of healthy foreskin fibroblast HFF cells, and so at all three time points and all concentrations. HFF did not express significant differences in fluorescence intensity at any of the temperatures and time conditions examined. All cells were incubated under the same conditions and shown no difference between HAL in PBS or in serum-free media (Fig. S6).

During the first 0.5 h of HAL application, the PpIX fluorescence was almost 2 times lower than after 2 h incubation at 37 °C, similarly to what was observed for cells in suspension (section 3.2). The difference in mean fluorescence intensities between HFF and HT1376 cells was highly statistically significant when incubated at 37 °C [95% CI p = 0.00008 (0.5 h), p = 0.00,002 (1 h), p = 0.000000002 (2 h)] and statistically different when incubated at room temperature [95% CI p = 0.00007 (0.5 h), p = 0.00,001 (1 h), p = 0.0000001 (2 h)]. Therefore, we concluded the best approach for use would be to incubate HAL at 37 °C for 2 h.

Several studies investigated how the temperature influences 5-ALA uptake and its conversion to PpIX *in vitro* or *in vivo*. Most of the previous *in vivo* research focused on skin cancer [42,44–46]. Their data proves that PpIX production in the skin cells is temperature dependent. No or little PpIX production occurs when the skin temperature was below 15 °C. In good agreement with the results presented here, these works reported that PpIX fluorescence increased as the temperature increased between 23 °C and 37 °C. Other research groups investigating different types of cancer cells monolayers *in vitro* also indicated that a rise in temperature increases the PpIX production [41,47]. Here we demonstrated for the first time that this trend also holds for cells in suspension which is an important finding for the future use of HAL in *ex-vivo* diagnosis of cancer from body fluids.

3.4. Effect of nuclear red

Nuclear red was chosen as a tool for the subcellular localization of PpIX. It is a cell-permeant nucleic acid detection dye which stains nuclei in live cells, and shows red fluorescence significantly enhanced upon binding to DNA. The fluorescence spectrum of PpIX and nuclear red are shown in Fig. 4a. The Soret band of the excitation spectrum has a maximum at 405 nm and emission at 635 nm for PpIX. However, nuclear red exhibits excitation at 622 nm and emission at 645 nm. As the excitation wavelength are well separated, there is no cross over from one fluorescent dye to the other when appropriate narrow band excitation filters are used (Fig. S8).

After 1 h of HAL incubation and 15 min nuclear red treatment in 37 °C, both bladder cancer HT1376 and HT1197 cells showed clear red fluorescence when observed in the nuclear red and HAL fluorescence channels. Fluorescence microscopy revealed that, while the nuclear red localised in the cell nucleus as expected, accumulated PpIX mainly

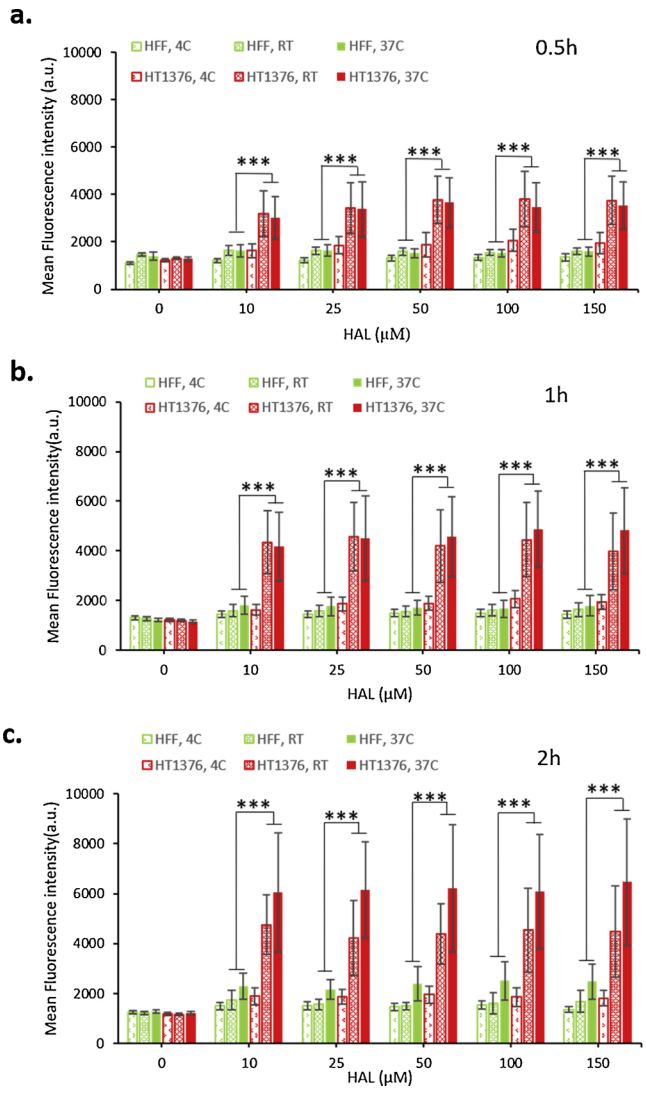

Fig. 3. Effect of temperature on PPIX fluorescence in bladder cancer HT1376 cells and human foreskin fibroblast cells after incubation with various concentrations of HAL in a) 0.5 h, b) 1 h and c) 2 h time. Note only for RT and 37 °C, *p*-value was calculated as *** $p < 0.001$.

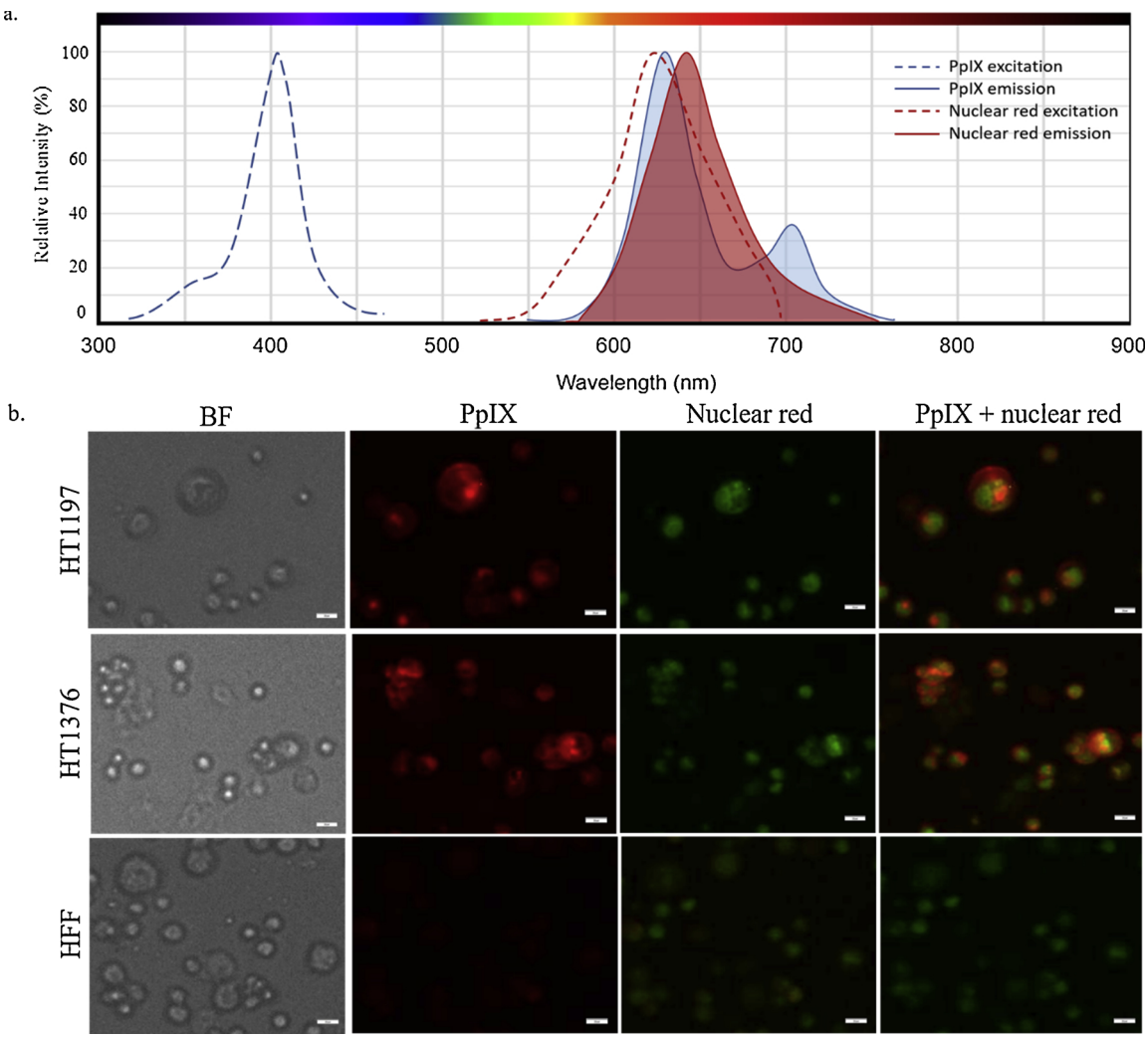

Fig. 4. PpIX and nuclear red. a) PpIX has an excitation at 405 nm and emission at 635 nm. Nuclear red has an excitation and emission at 622 nm and 645 nm respectively. Nuclear red increased cancer cell sensitivity to PpIX accumulation after HAL incubation. b) Fluorescence microscopy images of different cell lines after incubation with HAL. Cells were incubated in serum-free medium with 50 μM HAL for 1 h. Cells were stained with 0.5 μM nuclear red for 15 min before observation. HAL-induced PpIX red fluorescence were observed in HT1197 and HT1376 cells but not in HFF cells. Original magnification 5 × .

localised in other cell organelles in both bladder cancer HT1197 and HT1376 cells (Fig. 4b). Based on current knowledge of the heme biosynthesis pathway, it is likely that PpIX is accumulating in the mitochondria, however, further investigation is warranted to confirm PpIX localisation and determine if it differs from one cell type to another.

Most remarkably, we observed that the addition of nuclear red increased, overtime, the specificity of the HAL-induced fluorescence towards cancer cells. Indeed, after 2 h HAL incubation, the accumulation of PpIX in both cancer HT1197 and HT1376 cells was markedly higher in cells treated with nuclear red than HAL alone. In contrast, the much less fluorescent HFF did not exhibit any difference in the presence or absence of nuclear red. Similar results were observed after just 1 h HAL incubation, but only for HT1376. (Fig. 5a.) Quantitatively, after 2 h incubation with 50 μM HAL, the PpIX fluorescence intensity increased by 20 and 30% for HT1197 and HT1376 cancer cells, respectively, when incubated with nuclear red. In the same conditions, no increase in fluorescence is observed for the healthy foreskin fibroblast HFF cells. Overall, the fluorescence of HT1376, was after 2 h incubation with 50 μM HAL and nuclear red, 4.5 times higher than that of healthy HFF (Fig. S9).

This result indicates that the post-treatment with nuclear red increased the PpIX accumulation specificity. It could therefore be used as an adjuvant to better discriminate between healthy and cancer cells. To shed light on the mechanism that could explain this enhanced cancer specificity, we investigated the cell viability in the relevant experimental conditions (HAL 50 μM, 1 h, and nuclear red 15 min incubation). Results are shown in Fig. 5b. Both HAL and nuclear red have moderate toxicity for HT1376 and HT1197. HFF, on the other hand, bear a 50% decrease in cell viability when treated with HAL and nuclear red. Interestingly, the % of viability for both cancer cell lines are slightly lower after 1 h HAL incubation alone.

The difference observed, in both viability and PpIX fluorescence, between cancer and healthy cell could be the result of distinctive enzymatic activities, which can in part be explained by existing literature investigating the heme biosynthesis pathway triggered by the administration of exogenous HAL. It has been shown that excess free heme causes the formation of cytotoxic lipid peroxide which increases membrane permeability and sequentially may trigger cell lysis and death [48,49]. Yet, at least two distinct aberrant enzymatic expression have been reported that could explain why heme production is hindered and PpIX accumulates in bladder cancer cells.

First, iron deficiency, or more precisely the lack of available mitochondrial iron is very common in cancer [49] and has been attributed, in bladder carcinoma, to low level of mitochondrial iron transporters Mitoferrin 1 and 2 [48,50]. Second, low levels of FECH -an

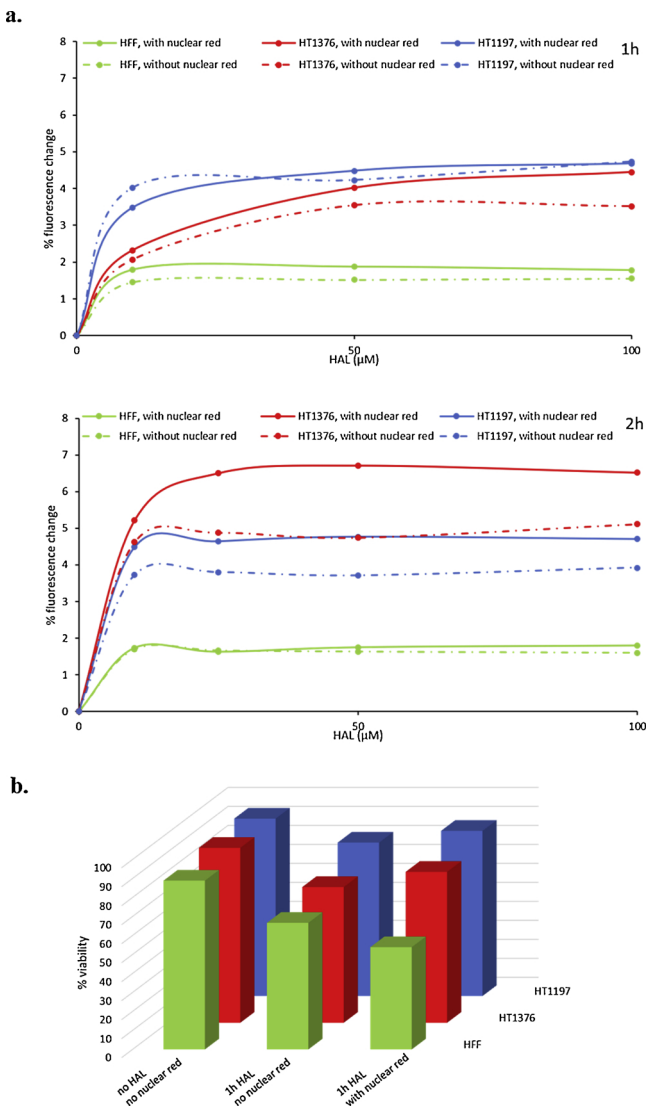

Fig. 5. Nuclear red. a) Effect of nuclear red on cell fluorescence intensity changes after 1 or 2 h incubated with various HAL concentrations in serum-free medium. Cells were measured under the SMR microscope. b) cell viability of cells after 1 h 50 μM HAL incubation with or without nuclear red staining, different types of cells were counted with the LUNA-II™.

enzyme that catalyzes the formation of heme through the integration of iron into PpIX, -has been reported for bladder cancer tissue [51,52]. Low FECH level means that PpIX accumulates rather forming peroxide triggering heme. Taken together, low level of FECH and iron could reduce the free heme toxicity in cancer cells compared to foreskin fibroblast HFF cells.

While the exact mechanism by which the nuclear red affected the PpIX production is not clear, the role played by the solvent DMSO should not be overlooked. DMSO is a highly membrane penetrative 5-ALA enhancer [53] but also acts as an iron chelator [54] in conjunction with 5-ALA. In fact, it has already been shown that DMSO [53–57] can enhance the 5-ALA-induced PpIX accumulation in cells. Our results further suggest that DMSO actually increases PpIX fluorescence in cancer cell more than in healthy cells, thus enhancing the specificity of HAL.

3.5. Cell capture experiment

The efficiency of HAL fluorescence at impartially discriminating between malignant and benign cells was then tested on immuno-captured cell populations. A microfluidic designed to isolate cells based on their over-expression of EpCAM was used as described previously. Both healthy foreskin fibroblast HFF and cancer cells were stained with HAL: 50 μM for 30 min. at 37 °C and 30 min. at 23 °C. In addition, the cancer cells were also stained with nuclear red, prior to mixing 1:1 both cell type in PBS. The mix suspensions of healthy and cancer cells were then dispensed inside three microfluidic channels (Fig. 6d), namely a negative control 'block' channel, a positive control 'plasma POx' coated channel, and the test channel functionalised with anti-EpCAM antibody. The cells were left to incubate on the different surfaces for 45 min before rinsing with PBS to dislodge any loosely bound cells. Images of the cells bound on the different surfaces inside the channels before and after PBS rinse were taken in bright field, and using custom fluorescent filters for PpIX and Cy5 (Nuclear red) fluorescence. The number of cells observed in bright field images correspond to the total number of cancer and non-cancer cells, while the number of cells observed with the Cy5 fluorescent filter correspond to cancer cells only. Finally, the number of fluorescent cells observed with the PpIX fluorescent filter, is used to determine the capacity of HAL at discriminating between healthy and cancer cells in the captured cell population.

The number of cells present in the channels before rinse as well as the number of cells captured in the 3 channels are shown in Fig. 6. Before rinse, the number of Cy5 positive cells (Fig. 6c, blue bars) correspond to the number of cells visible in the PpIX optical channel (Fig. 6b, blue bars). Since non-cancer cells were not stain with Nuclear red, these results confirms that the cells visible and accounted for with the PpIX optical filters are indeed cancer cells. It further confirms that the healthy cells did not produced detectable intensity of PpIX fluorescence after HAL-treatment.

After rinse, for all optical filters, less than 3% of the cells remained bound to the block surface and more than 95% of the cell population remain bound to the POx coated channel, thus indicating that both negative and positive control surfaces performed as expected.

The channel functionalized with anti-EpCAM antibody captured 87% of the cells stained with Nuclear red, demonstrating that the selective capture of cancer cell was successful. Most importantly, when observed through the PpIX filter, an 88% capture rate was also achieved.

A histogram representing the mean statistical distribution of the PpIX fluorescence intensity in anti-EpCAM functionalized channels before and after wash is shown in Fig. 6e. The peak of the intensity profile occurs at higher fluorescence intensity after rinse than before (2100 and 1850 a.u., respectively). This is in good agreement with the results presented above which indicated that the PpIX fluorescence intensity increases from 1 to 2 h incubation time. Since the fluorescence intensity of foreskin fibroblast HFF is shifted towards lower values (Fig. S10), fitting the cell fluorescence intensity histograms could be used to impartially determine the nature of the captured cells.

Together, these results show that the immuno-capture platform is highly selective towards cancer cells and that HAL-induced PpIX fluorescence can be used to gain a second level of confidence on the malignant nature of the captured cell population. In fact, combining the selective immune-capture platform to the cancer specific HAL-induced PpIX accumulation allow for single cells to be individually identified in the microfluidic device, Fig. 6e.

4. Conclusion

Overall, our findings show that the HAL-induced fluorescence markedly increased in cancer cells compared to non-cancer cells regardless of whether these were cells in a monolayer or cells in suspension. Optimal conditions for achieving the best discrimination between cancer and healthy cell fluorescence were with cells in suspension incubated with 50 μM HAL in 37 °C for 2 h and followed by nuclear red treatment. This fluorescent technique has been successfully optimised and applied to the capture and detection of bladder cancer

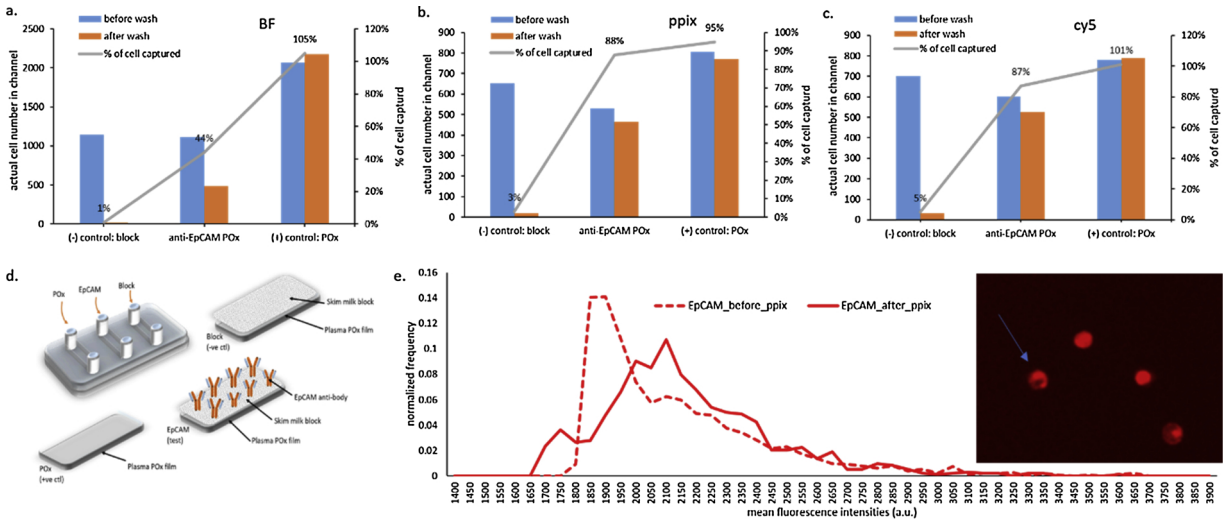

Fig. 6. Specific capture rate and actual cell number in microchannels of all substrates in a) bright field; b) PpIX; and c) cy5 filter. d) Schematic of the functionalized microchannel slide for cell capture experiment. Histogram data from the PpIX fluorescence images of anti-EpCAM functionalized substrate before and after wash and image of single cell captured *via*EpCAM affinity and PpIX positive was shown in e).

cells with a high 88% capture rate. This represents an attractive method for diagnosing the presence of bladder cancer cells in urine which can now be tested for performance as a diagnostic test in urine from patients with suspected bladder cancer or who are undergoing follow up surveillance.

Authors' contributions

MM designed, coordinated and supervised this research, wrote the manuscript. KMC designed and performed experiments, carried out data analysis, interpreted the data, wrote the manuscript. HSS and KM contributed reagents, and performed experiments. KV, JL and JG coordinated and supervised the research. The authors read and approved the final manuscript.

Declaration of Competing Interest

MM, JL, KV and JG are inventors on patents seeking to capture cancer cells from urine.

Appendix A. Supplementary data

Supplementary material related to this article can be found, in the online version, at doi:https://doi.org/10.1016/j.pdpdt.2019.08.001.

References

[1] Bethesda, SEER Cancer Stat Facts: Bladder Cancer, M. National Cancer Institute, 2018, https://seer.cancer.gov/statfacts/html/urinb.html.
[2] R.L. Siegel, K.D. Miller, A. Jemal, Cancer Statistics, 2017, CA Cancer J. Clin. 67 (1) (2017) 7–30.
[3] J.A. Witjes, The impact of recurrent non-muscle-invasive bladder cancer on progression, Eur. Urol. 63 (1) (2013) 155–157.
[4] J. Leal, R. Luengo-Fernandez, R. Sullivan, J.A. Witjes, Economic burden of bladder Cancer Across the european union, Eur. Urol. 69 (3) (2016) 438–447.
[5] B. Geavlete, R. Multescu, D. Georgescu, M. Jecu, F. Stanescu, P. Geavlete, Treatment changes and long-term recurrence rates after hexaminolevulinate (HAL) fluorescence cystoscopy: does it really make a difference in patients with non-muscle-invasive bladder cancer (NMIBC)? BJU Int. 109 (4) (2012) 549–556.
[6] M.D.Y. Bell, F.A, F. Brimo, J. Steinberg, A.G. Aprikian, S. Tanguay, W. Kassouf, Prognostic value of urinary cytology and other biomarkers for recurrence and progression in bladder cancer: a prospective study, World J. Urol. 34 (2016) 1405–1409.
[7] M. Kriegmair, A. Ehsan, R. Baumgartner, W. Lumper, R. Knuechel, F. Hofstädter, P. Steinbach, A. Hofstetter, Fluorescence photodetection of neoplastic urothelial lesions following intravesical instillation of 5-aminolevulinic acid, Urology 44 (6) (1994) 836–841.
[8] P. Steinbach, H. Weingandt, R. Baumgartner, M. Kriegmair, F. Hofstadter, R. Knuchel, Cellular fluorescence of the endogenous photosensitizer protoporphyrin IX following exposure to 5-aminolevulinic acid, Photochem. Photobiol. 62 (5) (1995) 887–895.
[9] P. Ponka, Cell biology of heme, Am. J. Med. Sci. 318 (4) (1999) 241–256.
[10] X. Yang, W. Li, P. Palasuberniam, K.A. Myers, C. Wang, B. Chen, Effects of silencing heme biosynthesis enzymes on 5-Aminolevulinic acid-mediated protoporphyrin IX fluorescence and photodynamic therapy, Photochem. Photobiol. 91 (4) (2015) 923–930.
[11] J.D. Spikes, The historical development of ideas on applications of photosensitized reactions in the health sciences, in: R.V. Bensasson, G. Jori, E.J. Land, T.G. Truscott (Eds.), Primary Photo-Processes in Biology and Medicine, Springer US, Boston, MA, 1985, pp. 209–227.
[12] J.C. Kennedy, R.H. Pottier, D.C. Pross, Photodynamic therapy with endogenous protoporphyrin IX: basic principles and present clinical experience, J. Photochem. Photobiol. Biol. 6 (1–2) (1990) 143–148.
[13] M. Kriegmair, R. Baumgartner, R. Knüchel, A. Ehsan, P. Steinbach, W. Lumper, F. Hofstädter, A. Hofstetter, Photodynamic diagnosis of urothelial neoplasms after intravesicular instillation of 5-aminolevulinic acid, Urologe A. 33 (4) (1994) 270–275.
[14] M.-A. D'Hallewin, L. Bezdetnaya, F. Guillemin, Fluorescence detection of bladder Cancer: a review, Eur. Urol. 42 (5) (2002) 417–425.
[15] P. Jichlinski, L. Guillou, S.J. Karlsen, P.-U. MalmstrÖM, D. Jocham, B. Brennhovd, E.V.A. Johansson, T. GÄRtner, N. Lange, H. van den Bergh, H.-J. Leisinger, Hexyl aminolevulinate fluorescence cystoscopy: a new diagnostic tool for photodiagnosis of superficial bladder cancer—a multicenter study, J. Urol. 170 (1) (2003) 226–229.
[16] A. Marti, P. Jichlinski, N. Lange, J.P. Ballini, L. Guillou, H.J. Leisinger, P. Kucera, Comparison of aminolevulinic acid and hexylester aminolevulinate induced protoporphyrin IX distribution in human bladder Cancer, J. Urol. 170 (2) (2003) 428–432.
[17] N. Lange, P. Jichlinski, M. Zellweger, M. Forrer, A. Marti, L. Guillou, P. Kucera, G. Wagnières, H. Bergh, Photodetection of early human bladder cancer based on the fluorescence of 5-aminolaevulinic acid hexylester-induced protoporphyrin IX: a pilot study, Br. J. Cancer 80 (1–2) (1999) 185–193.
[18] M.H. Abdel-Kader, History of photodynamic therapy, in: M.H. Abdel-Kader (Ed.), Photodynamic Therapy: From Theory to Application, Springer Berlin Heidelberg, Berlin, Heidelberg, 2014, pp. 3–22.
[19] L. Rodriguez, A. Batlle, G. Di Venosa, S. Battah, P. Dobbin, A.J. Macrobert, A. Casas, Mechanisms of 5-aminolevulinic acid ester uptake in mammalian cells, Br. J. Pharmacol. 147 (7) (2006) 825–833.
[20] S. Daneshmand, S. Patel, Y. Lotan, K. Pohar, E. Trabulsi, M. Woods, T. Downs, W. Huang, J. Jones, M. O'Donnell, T. Bivalacqua, J. DeCastro, G. Steinberg, A. Kamat, M. Resnick, B. Konety, M. Schoenberg, J.S. Jones, Efficacy and Safety of Blue Light Flexible Cystoscopy with Hexaminolevulinate in the Surveillance of Bladder Cancer: A Phase III, Comparative, Multicenter Study, J. Urol. 199 (5) (2018) 1158–1165.
[21] B. Čunderlíková, R. Wahlqvist, A. Berner, V. Vasovič, T. Warloe, J.M. Nesland, Q. Peng, Detection of urinary bladder cancer with flow cytometry and hexaminolevulinate in urine samples, Cytopathology 18 (2) (2007) 87–95.
[22] M. Ishizuka, Y. Hagiya, Y. Mizokami, K. Honda, K. Tabata, T. Kamachi, K. Takahashi, F. Abe, T. Tanaka, M. Nakajima, S. Ogura, I. Okura, Porphyrins in urine after administration of 5-aminolevulinic acid as a potential tumor marker, Photodiagnosis Photodyn. Ther. 8 (4) (2011) 328–331.
[23] M. Miyake, Y. Nakai, S. Anai, Y. Tatsumi, M. Kuwada, S. Onishi, Y. Chihara, N. Tanaka, Y. Hirao, K. Fujimoto, Diagnostic approach for cancer cells in urine sediments by 5-aminolevulinic acid-based photodynamic detection in bladder

cancer, Cancer Sci. 105 (5) (2014) 616–622.
[24] Y. Nakai, T. Ozawa, F. Mizuno, S. Onishi, T. Owari, S. Hori, Y. Morizawa, Y. Tatsumi, M. Miyake, N. Tanaka, D. Tsuruta, K. Fujimoto, Spectrophotometric photodynamic detection involving extracorporeal treatment with hexaminolevulinate for bladder cancer cells in voided urine, J. Cancer Res. Clin. Oncol. 143 (11) (2017) 2309–2316.
[25] N. Fotinos, M. Convert, J.C. Piffaretti, R. Gurny, N. Lange, Effects on gram-negative and gram-positive bacteria mediated by 5-aminolevulinic Acid and 5-aminolevulinic acid derivatives, Antimicrob. Agents Chemother. 52 (4) (2008) 1366–1373.
[26] C.Y. Fu, B.K. Ng, S.G. Razul, W.W. Chin, P.H. Tan, W.K. Lau, M. Olivo, Fluorescence detection of bladder cancer using urine cytology, Int. J. Oncol. 31 (3) (2007) 525–530.
[27] M. Macgregor-Ramiasa, K. McNicholas, K. Ostrikov, J. Li, M. Michael, J.M. Gleadle, K. Vasilev, A platform for selective immuno-capture of cancer cells from urine, Biosens. Bioelectron. 96 (Supplement C) (2017) 373–380.
[28] O. Dragoescu, P. Tomescu, A. Panus, M. Enache, C. Maria, L. Stoica, I.E. Plesea, Photodynamic diagnosis of non-muscle invasive bladder cancer using hexaminolevulinic acid, Rom. J. Morphol. Embryol. 52 (1) (2011) 123–127.
[29] M.N. Ramiasa, A.A. Cavallaro, A. Mierczynska, S.N. Christo, J.M. Gleadle, J.D. Hayball, K. Vasilev, Plasma polymerised polyoxazoline thin films for biomedical applications, Chem. Commun. 51 (20) (2015) 4279–4282.
[30] M.N. Macgregor-Ramiasa, A.A. Cavallaro, K. Vasilev, Properties and reactivity of polyoxazoline plasma polymer films, J. Mater. Chem. B 3 (30) (2015) 6327–6337.
[31] L.E. Gonzalez Garcia, M. MacGregor-Ramiasa, R.M. Visalakshan, K. Vasilev, Protein interactions with nanoengineered polyoxazoline surfaces generated via plasma deposition, Langmuir 33 (29) (2017) 7322–7331.
[32] H.G. Stepp, R. Baumgartner, W. Beyer, R. Knuechel, K. Rick, P. Steinbach, M. Kriegmair, Bladder Tissue Diagnostics Utilizing Protoporphyrin IX Fluorescence Detection, International Symposium on Biomedical Optics Europe' 94, SPIE, 1995, p. 12.
[33] M. MacGregor, U. Sinha, R.M. Visalakshan, A. Cavallaro, K. Vasilev, Preserving the reactivity of coatings plasma deposited from oxazoline precursors − an in depth study, Plasma Process. Polym. 16 (2) (2019) 1800130.
[34] J. Moan, O. Bech, J.M. Gaullier, T. Stokke, H.B. Steen, L.W. Ma, K. Berg, Protoporphyrin IX accumulation in cells treated with 5-aminolevulinic acid: dependence on cell density, cell size and cell cycle, Int. J. Cancer 75 (1) (1998) 134–139.
[35] A. Casas, H. Fukuda, G. Di Venosa, A. Batlle, Photosensitization and mechanism of cytotoxicity induced by the use of ALA derivatives in photodynamic therapy, Br. J. Cancer 85 (2) (2001) 279–284.
[36] H. Kobuchi, K. Moriya, T. Ogino, H. Fujita, K. Inoue, T. Shuin, T. Yasuda, K. Utsumi, T. Utsumi, Mitochondrial localization of ABC transporter ABCG2 and its function in 5-Aminolevulinic acid-mediated protoporphyrin IX accumulation, PLoS One 7 (11) (2012) e50082.
[37] N. Rosenberg, O. Rosenberg, A. Weizman, L. Veenman, M. Gavish, In vitro catabolic effect of protoporphyrin IX in human osteoblast-like cells: possible role of the 18 kDa mitochondrial translocator protein, J. Bioenerg. Biomembr. 45 (4) (2013) 333–341.
[38] Z. Yang, J.D. Philips, R.T. Doty, P. Giraudi, J.D. Ostrow, C. Tiribelli, A. Smith, J.L. Abkowitz, Kinetics and specificity of feline leukemia virus subgroup C receptor (FLVCR) export function and its dependence on hemopexin, J. Biol. Chem. 285 (37) (2010) 28874–28882.
[39] C.V. Dang, Links between metabolism and cancer, Genes Dev. 26 (9) (2012) 877–890.
[40] R.J. DeBerardinis, N.S. Chandel, Fundamentals of cancer metabolism, Sci. Adv. 2 (5) (2016) e1600200.
[41] J. Moan, K. Berg, Ø. Gadmar, V. Iani, L. Ma, P. Juzenas, The temperature dependence of protoporphyrin IX production in cells and tissues, Photochem. Photobiol. 70 (4) (1999) 669–673.
[42] J.T.H.M. van den Akker, K. Boot, D.I. Vernon, S.B. Brown, L. Groenendijk, G.C. van Rhoon, H.J.C.M. Sterenborg, Effect of elevating the skin temperature during topical ALA application on in vitro ALA penetration through mouse skin and in vivo PpIX production in human skin, Photochem. Photobiol. Sci. 3 (3) (2004) 263–267.
[43] A. Willey, R.R. Anderson, F.H. Sakamoto, Temperature-modulated photodynamic therapy for the treatment of actinic keratosis on the extremities: a pilot study, Dermatol. Surg. 40 (10) (2014) 1094–1102 [et al.].
[44] A. Juzeniene, P. Juzenas, O. Kaalhus, V. Iani, J. Moan, Temperature effect on accumulation of protoporphyrin IX after topical application of 5-aminolevulinic acid and its methylester and hexylester derivatives in normal mouse skin, Photochem. Photobiol. 76 (4) (2002) 452–456.
[45] J. Yang, A.C.-H. Chen, Q. Wu, S. Jiang, X. Liu, L. Xiong, Y. Xia, The influence of temperature on 5-aminolevulinic acid-based photodynamic reaction in keratinocytes in vitro, Photodermatology, Photoimmunology & Photomedicine 26 (2) (2010) 83–88.
[46] A. Mamalis, E. Koo, G.D. Sckisel, D.M. Siegel, J. Jagdeo, Temperature-dependent impact of thermal aminolaevulinic acid photodynamic therapy on apoptosis and reactive oxygen species generation in human dermal fibroblasts, Br. J. Dermatol. 175 (3) (2016) 512–519.
[47] E. Rud, O. Gederaas, A. Hogset, K. Berg, 5-aminolevulinic acid, but not 5-aminolevulinic acid esters, is transported into adenocarcinoma cells by system BETA transporters, Photochem. Photobiol. 71 (5) (2000) 640–647.
[48] P.N. Paradkar, K.B. Zumbrennen, B.H. Paw, D.M. Ward, J. Kaplan, Regulation of mitochondrial iron import through differential turnover of mitoferrin 1 and mitoferrin 2, Mol. Cell. Biol. 29 (4) (2009) 1007–1016.
[49] H. Ludwig, E. Müldür, G. Endler, W. Hübl, Prevalence of iron deficiency across different tumors and its association with poor performance status, disease status and anemia, Ann. Oncol. 24 (7) (2013) 1886–1892.
[50] M. Hayashi, H. Fukuhara, K. Inoue, T. Shuin, Y. Hagiya, M. Nakajima, T. Tanaka, S. Ogura, The effect of iron ion on the specificity of photodynamic therapy with 5-aminolevulinic acid, PLoS One 10 (3) (2015) e0122351.
[51] Y. Hagiya, H. Fukuhara, K. Matsumoto, Y. Endo, M. Nakajima, T. Tanaka, I. Okura, A. Kurabayashi, M. Furihata, K. Inoue, T. Shuin, S. Ogura, Expression levels of PEPT1 and ABCG2 play key roles in 5-aminolevulinic acid (ALA)-induced tumor-specific protoporphyrin IX (PpIX) accumulation in bladder cancer, Photodiagnosis Photodyn. Ther. 10 (3) (2013) 288–295.
[52] Y. Nakai, Y. Tatsumi, M. Miyake, S. Anai, M. Kuwada, S. Onishi, Y. Chihara, N. Tanaka, Y. Hirao, K. Fujimoto, Expression of ferrochelatase has a strong correlation in protoporphyrin IX accumulation with photodynamic detection of bladder cancer, Photodiagnosis Photodyn. Ther. 13 (Supplement C) (2016) 225–232.
[53] F.S. De Rosa, J.M. Marchetti, J.A. Thomazini, A.C. Tedesco, M.V.L.B. Bentley, A vehicle for photodynamic therapy of skin cancer: influence of dimethylsulphoxide on 5-aminolevulinic acid in vitro cutaneous permeation and in vivo protoporphyrin IX accumulation determined by confocal microscopy, J. Control. Release 65 (3) (2000) 359–366.
[54] L.H. Conder, S.I. Woodard, H.A. Dailey, Multiple mechanisms for the regulation of haem synthesis during erythroid cell differentiation. Possible role for coproporphyrinogen oxidase, Biochem. J. 275 (Pt 2) (1991) 321–326.
[55] Z. Malik, G. Kostenich, L. Roitman, B. Ehrenberg, A. Orenstein, Topical application of 5-aminolevulinic acid, DMSO and EDTA: protoporphyrin IX accumulation in skin and tumours of mice, J. Photochem. Photobiol. B, Biol. 28 (3) (1995) 213–218.
[56] A. Casas, C. Perotti, H. Fukuda, L. Rogers, A.R. Butler, A. Batlle, ALA and ALA hexyl ester-induced porphyrin synthesis in chemically induced skin tumours: the role of different vehicles on improving photosensitization, Br. J. Cancer 85 (11) (2001) 1794–1800.
[57] L.-W. Zhang, Y.-P. Fang, J.-Y. Fang, Enhancement techniques for improving 5-aminolevulinic acid delivery through the skin, Dermatol. Sin. 29 (1) (2011) 1–7.